Blending with Non-responsive Polymers to Incorporate Nanoparticles into Shape-Memory Materials and Enable Photothermal Heating: The Effects of Heterogeneous Temperature Distribution

David B. Abbott, Somsubhra Maity, Mary T. Burkey, Russell E. Gorga, Jason R. Bochinski, Laura I. Clarke*

Blending a shape-memory polymer (SMP) (e.g., thermoplastic polyurethane) with an immiscible carrier polymer (e.g., poly(ethylene oxide) (PEO) or poly(vinyl alcohol) (PVA)) containing dispersed metal nanoparticles (AuNPs) is a simple approach to enable actuation via photothermal heating. For blends containing up to 90% carrier polymer, the shape-memory capability can be thermally triggered either conventionally or utilizing internal heating via application of light that is resonant with the particle's surface plasmon resonance. When incorporating nanoparticles in this manner, neither chemical modification of the shape-memory moiety nor solvation of the SMP is necessary. Actuation times are determined by the particular heterogeneous temperature distribution, which generally occurs under both conventional and photothermal heating methods, but with different spatial patterns. Blending an SMP with PEO containing AuNPs imposes a higher transition temperature (the melting point of PEO), enabling heat generated within the nanoparticle-containing regions to equilibrate throughout the sample, resulting in performance under photothermal conditions comparable with that achieved in a conventional heating approach. SMP:PVA blends actuate at the SMP transition temperature and the response depends on the size of phase segregation between the PVA and SMP; when decreasing the characteristic size of the segregated regions, heat is efficiently transferred and optimal photothermal performance is observed.

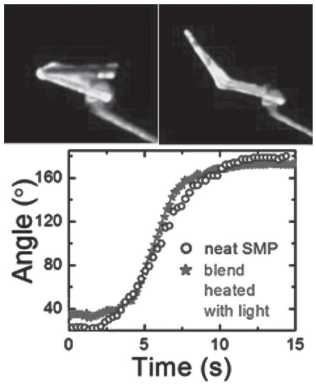

D. B. Abbott, Dr. S. Maity, M. T. Burkey, Prof. J. R. Bochinski, Prof. L. I. Clarke
Department of Physics, North Carolina State University, Box 8202, Raleigh, NC 27695–8202, USA
E-mail: liclarke@ncsu.edu
Prof. R. E. Gorga
Fiber and Polymer Science Program, North Carolina State University, Box 8301, Raleigh, NC 27695–8301, USA

1. Introduction

Shape-memory polymers (SMPs) can be programmed to perform one-time actuation when exposed to heat or another stimulus.[1] Most commonly, SMPs are block copolymers that contain a soft segment phase possessing a relatively low glass transition temperature ($T_{g,\,soft}$) and a

DOI: 10.1002/macp.201400386

hard segment phase that has a higher T_g ($T_{g,\ hard}$).[2] In the programming temperature range $T_{g,\ soft} < T < T_{g,\ hard}$, the sample can be intentionally conformed to a non-equilibrium shape (resulting, for instance, in chain alignment and elongation within the hard segment region), which upon cooling ($T < T_{g,\ soft}$) is stabilized by the glassy soft segments. When subsequently heated above the transition temperature ($T > T_{g,\ soft}$) where the soft segment again becomes rubbery, the sample relaxes to the originally fabricated equilibrium shape. Throughout the paper, the term "soft" component is associated with the transitioning region or segment, which is relaxed during setting and again relaxes/melts to allow actuation. "Hard" components which are still rigid/glassy during setting provide the force that restores the sample to its equilibrium shape when the reinforcing effect of the soft segment is removed above T_{soft}.

Interest in the shape-memory effect[1,3] continues to expand with new commercial applications including toothed-fasteners that release upon heating[4] and labels that reveal distinctive authentication patterns[5] adding to existing biomedical technologies, such as reactive sutures[6] and stents.[7] Thermally responsive SMPs have intrinsic disadvantages when actuating via conventional heating including accidental triggering, warming of the surroundings, and an inefficient use of energy. For many applications, a significant advantage may be realized by utilizing the photothermal effect of embedded metal nanoparticles to actuate SMP.[8–10] In nanoparticle-mediated photothermal processes, the particle's surface plasmon resonance (SPR) strongly absorbs incident light, which is converted into heat, resulting in an increase in particle temperature and the temperature of the surrounding polymer.[11] Because the surface-plasmon-mediated photothermal effect is a highly efficient, wavelength-specific process, significant heating can be accomplished with relatively low intensity irradiation. The maximum SPR wavelength can be tuned to an absorption minimum of the surrounding material through appropriate selection of the particle composition, size, and aspect ratio. Thus, embedding low concentrations of metal nanoparticles (i.e., less than a few weight percent (wt%)) within polymeric materials potentially enables internal heating of the polymer (e.g., up to hundreds of °C).[5,12,13] In this work, spherical gold nanoparticles (AuNPs) with a relatively narrow distribution (32 ± 8 nm) were used as the photothermal heaters.

Incorporating particles as externally controlled nanoscale heaters within SMP enables wavelength-specific heating: such a method eliminates accidental thermal triggering and allows heating without significantly warming the surroundings (even for material in direct contact with the heated composite),[13] which are particularly important advantages for biomedical and defense-sector applications. Photothermal heating is more specific (wavelength and orientation sensitive)[13] than induction heating of magnetic nanoparticles[14] and does not require a strong magnetic field. In the composite approach described here, no synthetic chemical modification of the SMP is necessary; rather the embedded particle determines the available wavelengths for heating and the shape-memory mechanism is still set and triggered by heat.

In order to utilize such a practical heating scheme, nanoparticles must be incorporated into the SMP. This is a particular challenge for metal particles (which are generally fabricated in solution and can degrade upon neat drying) and has limited photothermal applications in thermoplastics. We point out that the overall efficiency of alternative photothermal processes due to doping with carbon nanomaterials or organic dyes is several orders of magnitude weaker than the metal nanoparticle effect. Previous published work has relied on in situ polymerization with the particles present,[8] which is a synthesis-intensive method that cannot be generally applied to a wide range of materials, or on solvating thermoplastic polymers,[9,15] which is only applicable to few commercial SMP. Here, a more general approach is introduced where the particles are placed within a non-responsive carrier polymer, which is then blended with the SMP. These phase-segregated blends show similar triggering characteristics as the pure SMP material and their response can be implemented using either conventional or photothermal heating methods.

The approach is demonstrated with blends comprised of up to 90% non-responsive polymer (10 wt% SMP), with the same blend composition but differing phase morphology, and with carrier polymers possessing glass and melt transitions either below (poly(ethylene oxide) (PEO)) or above (poly(vinyl alcohol) (PVA)) the SMP transition temperature. We address the observed changes in response magnitude, quiescence time (i.e., time after heat is applied before any movement), and characteristic response time as a function of the blend properties (e.g., type and concentration) and differences due to photothermal and conventional actuation. The heterogeneous temperature distribution (different temperatures at different positions within the sample) present in both heating schemes is discussed. Simple models of the blends' thermal and mechanical properties are utilized to form a cohesive picture of the response of a polyurethane-based SMP under these conditions. These results should be broadly applicable to a variety of particle-based heating schemes and provide further understanding of the important heat transport issues within such useful blends. For sufficiently intimate blending with PVA, the response under photothermal heating could be identically matched with that of the neat SMP heated conventionally, reflecting no loss in performance and the enhanced ability to heat via light.

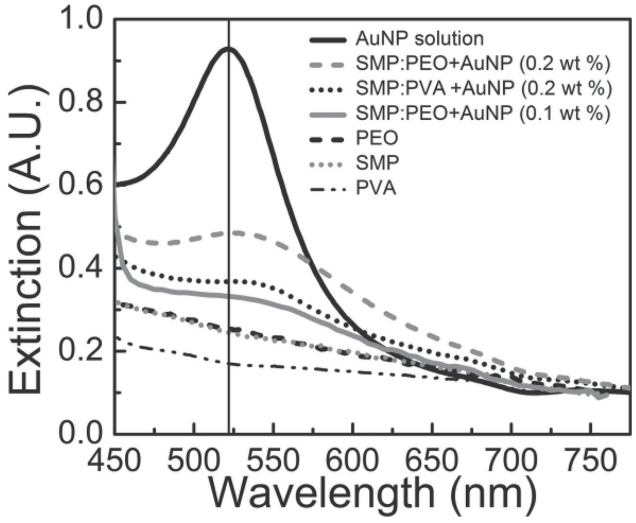

Figure 1. Normalized extinction spectra for different sample types. The vertical line is at 522 nm. No polymer films (PEO, PVA, and SMP) show any distinctive absorptive features in this region. The absorption peak of the as-fabricated AuNP in solution (water), of SMP:PEO films with 0.1 and 0.2 wt% of AuNPs:carrier polymer, and of SMP:PVA films is 522 ± 3, 530 ± 10, 525 ± 3, and 526 ± 3 nm.

2. Results and Discussion

2.1. Optical Properties

For the spherical AuNPs utilized in this work, the SPR peaks at ≈525 nm (Figure 1, AuNP solution).[16,17] Solid-phase samples of SMP:PEO or SMP:PVA containing AuNPs (gray dashed line and black dotted line, respectively) display the same spectral feature (little or no shift in the peak location), indicating no significant nanoparticle aggregation.[16,18] The spectra for pure SMP, pure PEO, and PVA (lines drawn with short dashes, gray dots, and dash–dot–dot symbols, respectively) are generally featureless.

2.2. Characterization of Phase Segregation

Optical images from characteristic nanoparticle-containing samples (0.2 wt% AuNPs:carrier polymer in 50:50 SMP:PEO, 50:50 SMP:PVA, and twice-mixed 50:50 SMP:PEO) are shown in Figure 2. All composite samples were macrophase-segregated with the AuNP-doped PEO or PVA regions remaining distinct from the SMP regions, as expected due to the poor miscibility of the carrier polymers and polyurethane. The AuNPs endow the carrier material phase with a reddish appearance due to the strong absorption of green light. Images of blended samples without nanoparticles were similar. The characteristic phase size in all standard fabricated samples was ≈0.5 mm. "Twice mixing" the samples (see Experimental Section) resulted in smaller phase size (≈0.1 mm) and less distinct macrophase separation (Figure 2e–h). Additionally, the incorporation of the fluorescent molecule perylene endows samples with a

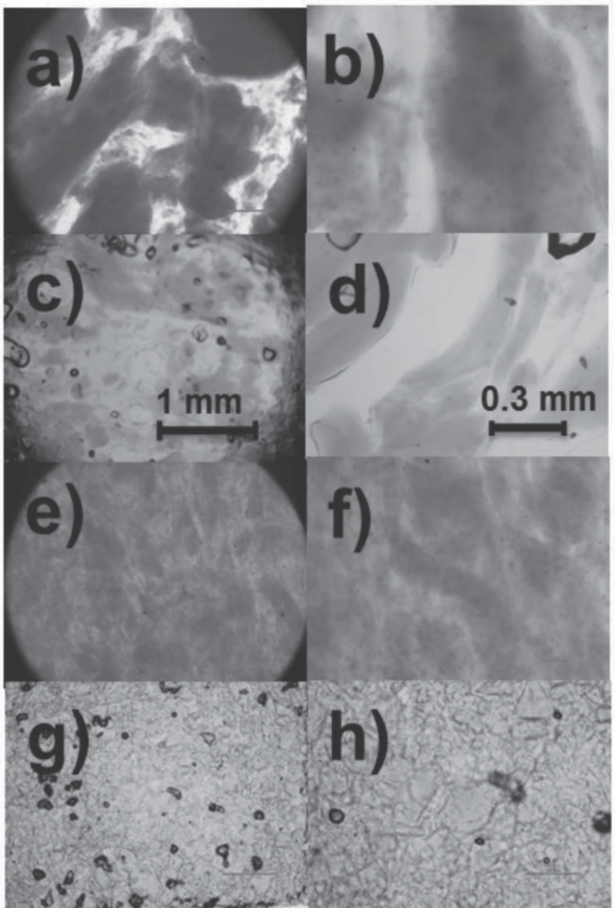

Figure 2. Optical images of a,b) 50:50 SMP:PEO (with 0.2 wt% AuNPs:PEO) samples fabricated in the standard manner or e,f) twice-mixed, and c,d) 50:50 SMP:PVA (with 0.2 wt% AuNPs:PVA) standard and g,h) twice-mixed samples. Scales for each column are given in the second row images.

light yellow color (due to absorption of violet-blue light), which was present in all phases, suggesting that the perylene is uniformly distributed throughout the sample. To determine if a mixed interphase of PEO (PVA) and SMP was present, optical images were analyzed by counting the number of filled (red, i.e. dark in greyscale image) pixels (Table 1). For all standard-fabricated samples, the observed areal fractions matched with expectations. Twice-mixed samples revealed a larger-than-expected AuNP-containing areal density, which may be indicative of a low level of AuNP migration from carrier regions to the SMP phases during the secondary regrinding step.

2.3. Shape-Memory Actuation

Figure 3a presents characteristic experimental data from a photothermally driven single actuation for a 50:50 SMP:PEO sample with 0.2 wt% AuNPs. The set, folded sample has a ≈30° initial angle (limited by the support clip, Figure 3b, i); angle is observed as a function of time

Table 1. Results of optical analysis quantifying the observed areal fraction associated with the carrier polymer phase (column 4). The first three columns specify the sample type including the expected carrier wt%. The areal fraction error is the standard deviation in the measured value from analysis of several images of each sample type.

Polymer blend	AuNPs:carrier polymer [wt%]	Carrier polymer:total polymer [wt%]	Areal fraction [%]
SMP	–	–	0.9 ± 0.2
PEO & SMP	–	50	51 ± 11
PEO & SMP	0.1	50	55 ± 6
PEO & SMP	0.2	50	60 ± 10
PEO & SMP[a)]	0.1	50	57 ± 4
PEO & SMP[a)]	0.2	50	62 ± 8
PVA & SMP	0.2	25	30 ± 8
PVA & SMP	0.2	33	37 ± 9
PVA & SMP	0.2	50	52 ± 5
PVA & SMP	0.2	90	92 ± 3
PVA & SMP[a)]	0.2	50	61 ± 6

[a)]Twice-mixed.

(Figure 3b, ii–iv). Upon illumination, there is a delay until the onset of motion (the quiescent time, B – A) followed by a characteristic time for sample actuation (the response time (C – B)/2), until ultimately a final angle is attained as the sample reverts to its initial flat shape. This general behavior occurred for all samples, with variation in the characteristic times and angles, depending upon the materials and conditions employed.

2.4. Heterogeneous Temperature Distributions in SMP under Conventional Heating

For oven temperatures of 70–91 °C, samples placed into a preheated oven begin to respond and usually complete actuation before reaching the equilibrium oven temperature. Figure 4 shows the bulk sample temperature at the instance of first movement for pure SMP 0.4-mm-thick film samples (open circles). At the beginning of actuation (e.g., at point B in Figure 3), the average sample temperature is 48 ± 1.5 °C regardless of the oven temperature. Previous studies of Tecoflex EG 72D[19] showed a soft segment $T_{g,\ soft}$ = 74 °C, with a sharp, order of magnitude decrease in storage modulus between 35 and 60 °C, consistent with the beginning of actuation at sample temperature $T \approx 50$ °C. Other studies on SMP "gated" or "switched" by a soft segment's glass transition have shown movement below $T_{g,soft}$, as this is not a sharp transition, with slower heating rates associated with lower temperatures at initial motion.[20] One effect of oven temperature is a decrease in the quiescent time (data not shown) – the time needed for the sample to warm to 48–49 °C – before the sample moves, with lower oven temperatures resulting in longer wait times. More importantly, response time was a function of oven temperature.

Figure 5a (open circles for pure SMP) displays the average temperature during actuation, which is also largely independent of oven settings, and ranges from 52 to 55 °C. In contrast, the response time (open black circles, Figure 5b) decreases with increasing oven temperature from 7.5 ± 1.8 s (T_{oven} = 70 °C) to 3.8 ± 0.4 s (T_{oven} = 91 °C), even though the bulk sample temperatures at the beginning of and during actuation are the same for all oven temperatures. In these cases, the surface of the film sample is likely at the oven temperature (70–91 °C), even though the bulk temperature has only warmed to ≈50 °C. The warmer sample regions result in faster dynamics and thus a decreased response time. This is an example of a particular locally heterogeneous temperature distribution (in this case, warmer on the surface, cooler in the interior) that occurs under conventional heating, and thus provides a useful comparison with the heterogeneous temperature patterns that are formed under photothermal heating as discussed below. Under conditions where the temperature is not spatially homogeneous, the overall dynamics of the actuation can be thought of as governed by an "effective dynamic temperature",[21] which has a value lying between the surface and bulk extremes.

Overall, SMP only samples responded at bulk temperatures of ≈50 °C with response time governed by surface temperature. Under all conditions, the pure SMP samples (0.3–0.4 mm thick, initial angle 31.0 ± 4° limited by the mounting clip) opened completely with an average final angle of 179.0 ± 2.5°.

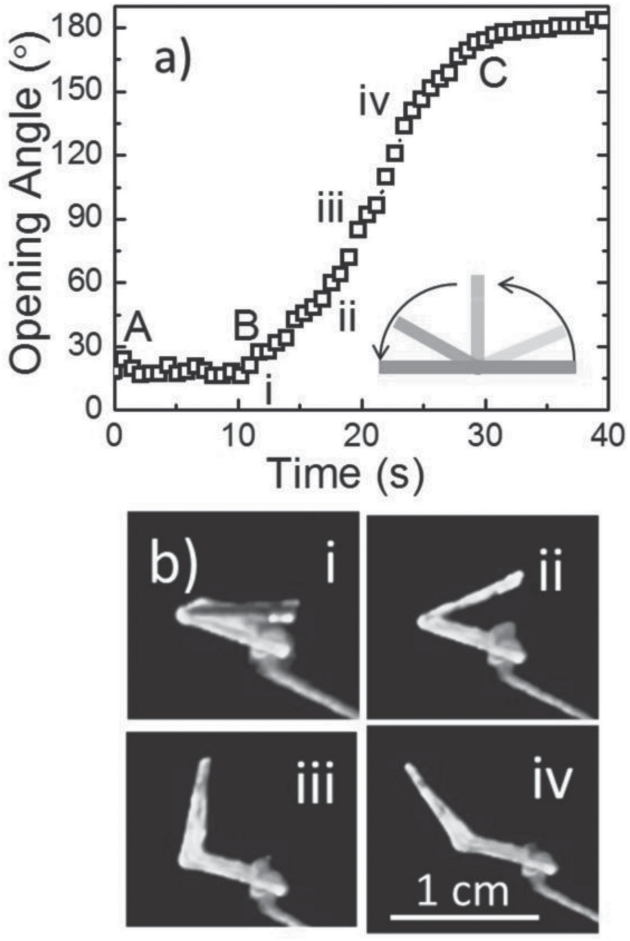

Figure 3. a) Angle versus time for actuation of film samples composed of 50:50 SMP:PEO containing 0.2 wt% AuNPs undergoing irradiation by 0.43 W cm^{-2} of 514 nm light. The sample is initially folded over (inset schematic) and straightens under photothermal application of heat. b) Sample images provided at indicated time points (i–iv) revealing characteristic motion. Scale bar is the same for all images.

2.5. Effect of Blending with PVA

Blending shape-memory polyurethane with other polymers will alter the samples' thermal and mechanical properties; to understand these changes, composite samples were tested under conventional heating for a direct comparison with the behavior of neat SMP films. The observed initial response temperatures for 50:50 SMP:PVA (0.2 wt% AuNPs) blends subjected to conventional heating are shown in Figure 4 (filled triangles). The SMP:PVA blends begin to actuate at similar temperatures as the neat SMP. Similarly, the response times and temperatures of such samples (Figure 5a,b, filled triangles) also overlap those for pure SMP. Mechanically, as compared with the composite PEO films, the 50:50 SMP:PVA samples were relatively rigid, possessing an average initial opening angle of 30 ± 11° and an average final angle of 170 ± 7°.

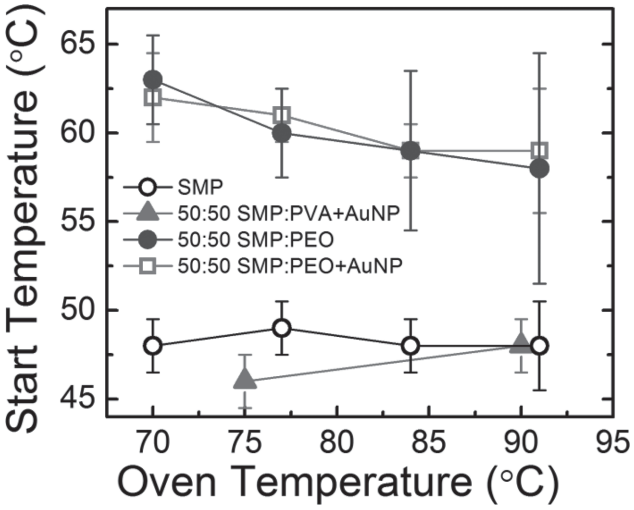

Figure 4. The measured bulk temperature at the moment actuation begins for composite film samples placed in a conventional oven at temperatures ranging from 70 to 91 °C. When present, AuNPs are at a concentration of 0.2 wt%. The error is determined from measurements of five different samples under the same conditions.

Altering the blend fraction from 10 to 90 wt% SMP had no effect on the quiescent time (Figure 6, filled triangles), and all samples types (blends (independent of concentration) and neat SMP) warmed at the same rate under the same oven conditions. This confirms the interpretation that the quiescent time is simply the wait required, while the sample warms from its ambient temperature to a level where actuation is possible. As might be expected due to the decrease in active, actuating polymeric fraction, the response (Figure 7, filled triangles) was slowed as the fraction of SMP decreased, yet response times were still within a factor of 2 of the neat SMP. In the most extreme case tested, 10:90 SMP:PVA samples had an average response time of 8.2 ± 2.0 s as compared with 4.9 ± 0.8 s for pure SMP under similar conditions. However, the final angle for samples with 90% PVA was only 127 ± 10°.

Thus, blending with PVA preserved the basic SMP response while easily incorporating nanoparticles that could be utilized for photothermal heating. These results are consistent with the nature of polyurethane SMP, which is a biphasic material even in neat form.[2] Hence, the PVA acts as either an additional inert component or adds to the "hard" phase fraction within the sample.[1,2] Samples are "set" at temperatures below or just approaching the T_g of PVA (≈85 °C); accordingly the PVA is still relatively rigid during the setting. In addition, in contrast to SMP:PEO blends (Section 2.6), the transition temperature of SMP:PVA blends is unaltered, indicating that PVA does not act as a "soft/switching" component.

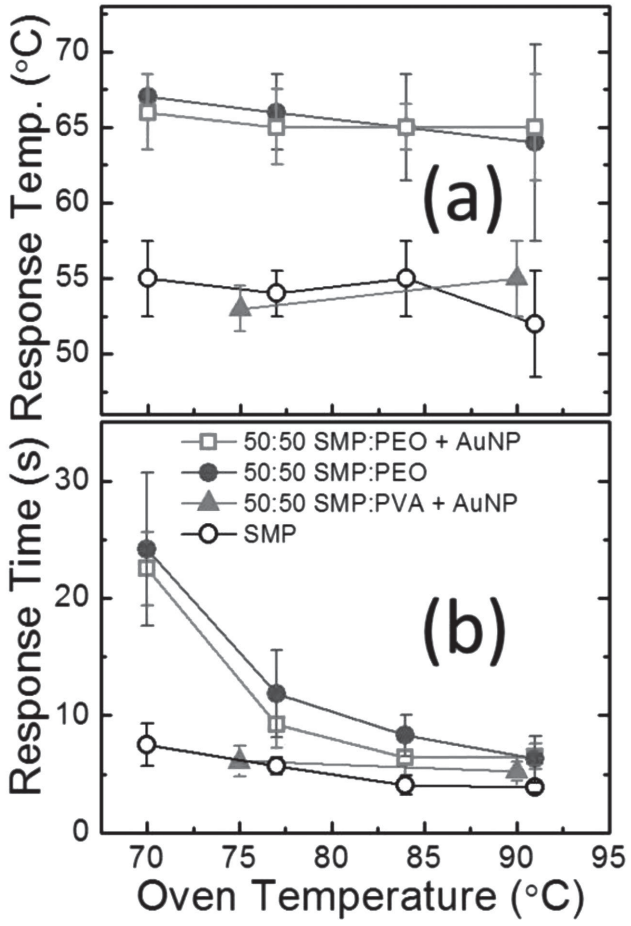

Figure 5. a) Response time and b) average bulk sample temperature during response for samples placed in an oven, undergoing conventional heating at temperatures ranging from 70 to 91 °C. When present, AuNPs are at a concentration of 0.2 wt%. The error is determined from measurements of five samples under the same conditions.

2.6. Effect of Blending with PEO

In some circumstances, PVA is known to have shape-memory ability;[1,22] in addition, the rigidity due to blending with a polymer in its glassy phase could hinder full actuation. PEO is a semicrystalline polymer (T_g = –67 °C, T_m = 65 °C) with amorphous regions, which remain in the rubbery phase at and above room temperature. PEO has a low barrier to crystallinity and possesses crystalline fractions >60% under most fabrication conditions.[23] Hence, PEO is likely to behave as either an inert load or serve as an additional "soft" or "switching" component within the sample, given that at the setting temperatures (70–80 °C for PEO:SMP samples), the PEO is above T_m.

SMP:PEO blends (50:50 SMP:PEO) displayed longer observed quiescent times (data not shown) and warmed to a higher temperature before actuation began compared with SMP:PVA or neat SMP. The bulk temperatures at the beginning of (averaging over all conditions 60 ± 2 °C) and during (Figure 5a (filled circles and open squares), on average 65.4 ± 1.6 °C) actuation are close to the PEO melting point (65 °C). Thus, this data suggest that the transition temperature of the SMP:PEO blends is increased to the PEO T_m. The contiguous PEO domains may "jam" the sample and mechanically prevent relaxation of elongated chains in the "hard" SMP domains until the PEO melt transition. PVA domains may, on average, be more isolated and less connected, which is more consistent with an inert or "hard" component (see Section 2.8).

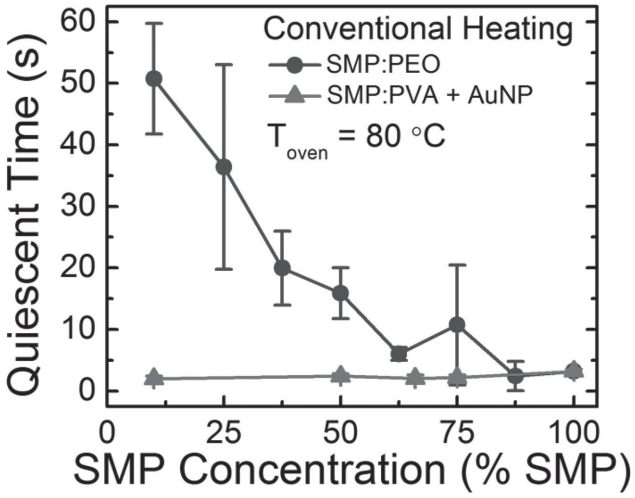

Figure 6. Quiescent time versus SMP concentration for 400 µm thick SMP:PEO and SMP:PVA samples annealed conventionally at T_{oven} = 80 °C. The error is determined from measurements of five samples under the same conditions. SMP:PVA samples have 0.2 wt% AuNPs:PVA.

The observed quiescent times for composite PEO blends are longer than for other sample types because the

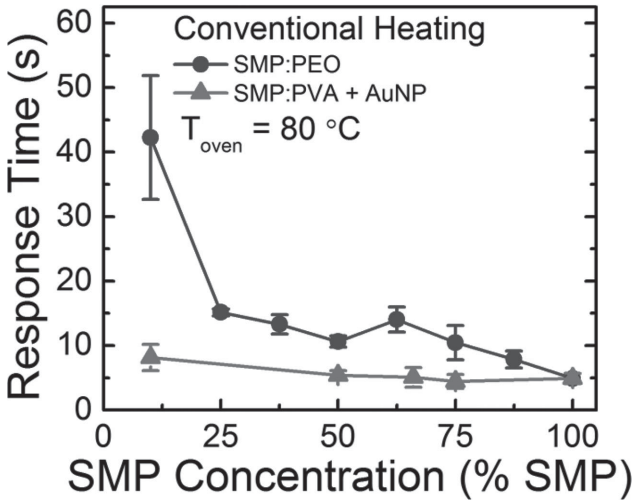

Figure 7. Response time versus SMP concentration for 400 µm thick SMP:PEO and SMP:PVA samples annealed conventionally at T_{oven} = 80 °C. The error is determined from measurements of five samples under the same conditions. SMP:PVA samples have 0.2 wt% AuNPs:PVA.

sample must warm to a higher temperature in order to actuate and because such samples have a slower rise in temperature with time, as expected due to the PEO phase transition. This intrinsic difference in heating rate is the most dramatic for T_{oven} = 70 °C; e.g., 50:50 SMP:PEO samples require about 15 s longer to attain a temperature of 66 °C than neat SMP samples in identical oven conditions. These trends are supported by quiescent time as a function of blend concentration (filled circles, Figure 6), which shows a dramatic increase in the delay time before movement as the PEO concentration is increased.

Heterogeneous temperature effects are also present in SMP:PEO blends. For an oven temperature of 70 °C, the blend samples warm nearly to the equilibrium temperature (a bulk temperature of 66–67 °C) during actuation, with a corresponding response time of 23.3 ± 3.6 s (filled circles and open squares, Figure 5b). This is the response time when the temperature is almost homogeneous throughout the sample. As the oven temperature is increased, the bulk temperature required for/during actuation remains within 1–2 °C of the PEO T_m, however, the surface temperature during actuation is significantly warmer, leading to faster responses. When the sample surface is at 91 °C, the response time has fallen to 6.4 ± 1.9 s, which is within a factor of 2 of the response of neat SMP under the same heating conditions and comparable with the response time of neat SMP in a 70 °C oven. Thus, the same general effect of heterogeneous temperature is present in both the blended and pure SMP samples.

Response times also provide an insight into the role of the PEO during the transition. For the 50:50 SMP:PEO samples in Figure 5, the bulk sample temperature is always warmer than the corresponding SMP sample and the surface temperatures are similar. However, the blended samples respond significantly more slowly. In contrast, the response time for a 50:50 SMP:PVA composite sample overlaps that of the pure SMP within error, and SMP:PVA blend response times only deviate significantly at the 10% SMP level. In fact, response times for a SMP:PEO composite at different blend ratios are always longer than the corresponding PVA blend, even though the fraction of the underlying responsive material (i.e., the SMP fraction) is the same in the two cases (Figure 7). Not only do SMP:PEO films have longer response times, they also possess a more dramatic change in response time with temperature than pure SMP samples, indicating the presence of a larger barrier to molecular motion, which is most logically associated with the PEO melting process. The significant fraction of immobile rigid crystallinity (for instance, spherulites of significant size)[21] is likely to significantly hinder actuation. Thus, all of the available time and temperature data support a self-consistent picture of the PEO, acting as a second "soft" phase material component. SMP:PEO blends set in the same manner as pure SMP samples (folded completely to 0° angle, which was opened to ≈30° for mounting) and fully actuated (final angle 175 ± 3° for 50:50 blend).

2.7. Response Under Photothermal Heating

To summarize the previous sections, based on the results from conventional heating, samples composed of SMP:PVA mixtures respond at bulk temperatures of ≈50–55 °C, where the PVA is either inert or has only a weak shape-memory effect. In contrast, SMP:PEO blends respond at bulk temperatures of ≈65 °C and the PEO acts as an additional soft/switching phase. Under photothermal heating, heat will be generated within the PEO or PVA phases at the nanoparticle locations and the SMP phases will only be warmed by conduction from these hotter material regions. Thus, the interior of the sample will be generally warmer than the surface and a heterogeneous temperature distribution will be present within the sample interior before it reaches equilibrium (just as in the conventional heating case but with a different spatial distribution of temperatures). As in the conventional case, shape-memory actuation occurs fully in the time before a final equilibrium temperature is established.

Under application of photothermal heating, the average sample temperature[5] can be tracked, which gives similar information as the bulk temperature measurement in the conventional heating case. However, under photothermal heating, the hottest temperature in the sample, which occurs locally at every photothermally heated particle rather than at the sample surface in the conventional approach, is not usually estimated or specifically measured. Previously, the authors have utilized rotation of an anisotropic particle as means to estimate the temperature in the local vicinity of the particle and compare it with the average sample temperature. Higher nanoparticle concentration and lower light intensity result in more homogeneous temperature distribution, that is, a smaller difference between the particle and background temperatures. As an example, experiments with varying wt% of gold nanorods in neat PEO under a constant irradiation intensity resulted in average background sample temperatures of ≈10–30 °C lower than the temperature in the immediate vicinity of the particle, once a steady-state equilibrium temperature is established.[5,12,13] Thus, the hottest temperature in the sample could be as low as 10 °C or as high as ≈30 °C above the bulk temperature.

2.7.1. SMP:PEO Response Under Photothermal Heating

Under photothermal heating, SMP:PEO samples (with either 0.1 or 0.2 wt% gold particles under three different heating conditions (0.3, 0.38, and 0.43 W cm^{-2}) that ultimately result in equilibrium temperatures of 79 ± 3, 85 ± 3,

and 94 ± 4 °C, averaging over all sample types) began to move and completed actuation at similar temperatures, irrespective of heating condition or sample type. Actuation started when the average sample temperature reached 37.5 ± 3.6 °C, accounting for all six experimental cases, which had overlapping errors. The average temperature during actuation was 62.5 ± 5.7 °C, which is fully consistent with the bulk temperature during actuation under conventional heating of 65 ± 2 °C. Thus, shape-memory action occurs only when the majority of the sample is at the PEO melt temperature, as discussed above. However, the lower temperature at the beginning of motion (compared with the analogous value under conventional heating of 60 ± 2 °C) reveals the greater temperature inhomogeneity internally present within the sample under photothermal heating (i.e., a larger temperature difference between the warmest and coldest regions), which may be particularly enhanced early in the heating process.

The average response times under photothermal heating varied from 44 ± 17 (0.1 wt% AuNPs at the lowest intensity) to 19 ± 6 s (0.2 wt% AuNPs at the highest intensity), with data from most conditions overlapping within error. Figure 8a summarizes response time for 50:50 SMP:PEO (0.2 wt% AuNPs) blends under different fabrication and heating conditions. The response time reflects an average dynamic temperature of the sample, which will fall in the range between the lowest and warmest temperatures at different spatial locations, with a value that will depend on the details on the particular spatial gradients in temperature. Comparing the analogous conventional experiments summarized above, photothermal response (Figure 8a, partially filled squares) is slower, which indicates the dynamic temperature is the same, or lower, under these photothermal conditions than in the conventional analogs. Such behavior is understandable because the warmest regions of the sample are within the PEO phase whereas the actuation is initiated in the SMP phase.

Comparing the temperature gradients in the two heating scenarios, the bulk temperature during actuation is similar (62–65 °C, as discussed above). On the other hand, the warmest temperatures in the photothermal case are expected to be at least ≈10 °C higher than the final steady-state average temperatures (as the particle itself should equilibrate very quickly and thus have a constant temperature with time) resulting in an estimated range from 80 to 105 °C, which is similar to but likely warmer than the hot surface in the conventional cases. Very warm temperatures at the nanoparticle are also consistent with the low-average sample temperature at which actuation begins. Thus, there is an innate balance between the temperature (higher) and location (less optimal) of the warmest regions when heating

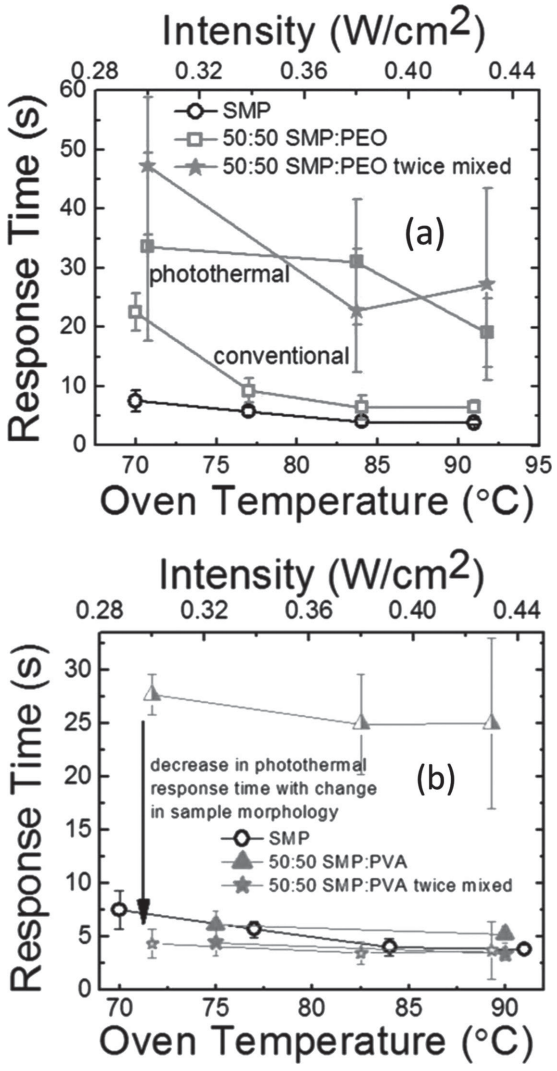

Figure 8. a) Response time versus oven temperature (lower axis, open squares and open circles) or laser intensity (upper axis, partially filled squares and stars) for neat SMP and 50:50 SMP:PEO samples fabricated with a standard (squares) or twice-mixed (stars) blending procedure. There is no difference in response under photothermal heating for different phase sizes (compare partially filled squares and stars). Photothermal heating at higher intensities results in response times similar to conventional heating in a 70 °C oven, which is close to the stated SMP transition temperature of 73 °C. Error is determined from measurements of five samples under the same conditions. b) Response time versus oven temperature (lower axis, filled triangles and open circles) or laser intensity (upper axis, partially filled triangles and stars) for neat SMP and 50:50 SMP:PVA samples fabricated with a standard (triangles) or twice-mixed (stars) blending procedure. For SMP:PVA samples with large phase-segregated regions, response time under photothermal heating is much slower than conventional actuation (difference between partially filled and fully filled triangles). In contrast for the smaller phase segregation (stars), the photothermally heated 50:50 blend performed as well as the pure SMP. The change in photothermal response time with smaller morphology is indicated by the black arrow. Error is determined from measurements of five samples under the same conditions.

photothermally from a blend. This challenge is addressed experimentally in Section 2.8. For 50:50 SMP:PEO (0.2 wt% AuNPs) sample, irradiation at the highest intensity resulted in a final opened angle of 161 ± 14°, which overlaps the average final angle (175 ± 3°) when heated conventionally.

2.7.2. SMP:PVA Response Under Photothermal Heating and Comparison of Blend Types

50:50 SMP:PVA (0.2 wt% AuNPs) blends began to respond within a few seconds of irradiation (independent of laser intensity), when the average temperature was still indistinguishable from room temperature (≈22 °C). The average temperature during actuation was 46 ± 5 °C, which overlaps the actuation temperature under conventional heating (54 ± 2 °C). However, response times for photothermal heating (Figure 8b, partially filled triangles) were much longer, an average of 26 ± 6 s compared with 5.6 ± 1.5 s when heated conventionally. Furthermore, the response time had no observable dependence on intensity in contrast with the PEO blend case, indicating that similar actuation times cannot be achieved under photothermal heating even at higher intensity. One plausible explanation for this result is that the SMP begins to respond at any location where the temperature is >≈50 °C even if the remainder of the sample is quite cold; these cold regions hinder the rate of actuation. Photothermally heated 50:50 SMP:PVA samples actuated as well as under conventional conditions with an average final angle of 158 ± 6° (compared with 170 ± 7° for conventional heating).

Comparing the two blend types, the PEO blends achieved performance with photothermal heating, which matched that under conventional heating at 70 °C. Thus, blending with such a soft phase is a generic approach that can be utilized to facilely incorporate nanoparticles into SMP for light-induced actuation. Efficient actuation under photothermal heating occurs because the PEO phase has two roles: acting as a source of heat and also representing a soft/switching phase that prevents actuation until the sample had warmed significantly. This delay enables heat to transfer throughout the sample from the heat source within the carrier PEO to the SMP, which results in warmer SMP regions, when the PEO finally melts and actuation can occur. Consequently, the relatively inefficient, piecemeal actuation (start of actuation when a large fraction of the sample is still cold) that occurs in the PVA blends is prevented. However, this argument suggests that a more intimate mixing of SMP and PVA might lead to improved performance, enabling a more homogenous temperature in the sample interior. Such results are discussed in Section 2.8.

2.8. Effect of Phase Segregation Changes

In order to further explore the effect of phase segregation, blends with a smaller characteristic phase size were fabricated (Figure 2e–h) and subjected to testing under photothermal heating. In these "twice-mixed" blends, the characteristic phase size is ≈0.1 mm and there is some evidence of AuNP migration into SMP regions or formation of an interphase of carrier and SMP (see Section 2.2). Twice-mixed SMP:PEO blends showed the same average temperature versus time curves under photothermal heating as standard analogs. In addition, the temperatures at the beginning (40 ± 5 °C) and during actuation (67 ± 7 °C), the range of response times, and the fastest response time (22 ± 10 s) match well with the results from samples with larger phases (see Section 2.7.1 and Figure 8a). For SMP:PEO samples of all types, the final angle increased with laser intensity. Comparing the highest intensity conditions, twice-blended samples (with either wt% of AuNPs) showed the same average final angle 172 ± 30° as the best responding standard SMP:PEO samples. These results indicate that the SMP:PEO samples are insensitive to phase size below 0.5 mm; performance is neither significantly degraded nor improved by enhanced blending.

In contrast, significant improvements were seen for SMP:PVA twice-mixed samples. Figure 8b summarizes response time as a function of sample fabrication and heating modality for 50:50 SMP:PVA samples. In contrast with standard fabricated samples, where the response time is dramatically longer when heating photothermally (comparing filled and partially filled triangle symbols), twice-mixed samples showed the same response time under either modality (closed and open star symbols) with times fully consistent with the response time of neat SMP (open circles). This result indicates that with sufficient mixing (small enough phase size), blended samples are able to perform as well as pure SMP samples. In fact, a direct comparison of photothermally heated 50:50 SMP:PVA samples with conventionally heated pure SMP samples (Figure 9) shows that response is almost identical. The optical images of twice-mixed samples (Figure 2g,h) are consistent with relatively isolated PVA regions embedded within contiguous SMP (rather than the explicitly co-contiguous PEO and SMP domains in the twice-mixed SMP:PEO samples, Figure 2e,f), which may provide heat to the SMP without altering its innate response. Thus, sufficient blending of the PVA and SMP enables photothermal heating with no loss in SMP performance. Twice-mixed SMP:PVA samples actuated equally well under all intensities with an average final angle of 163 ± 10°.

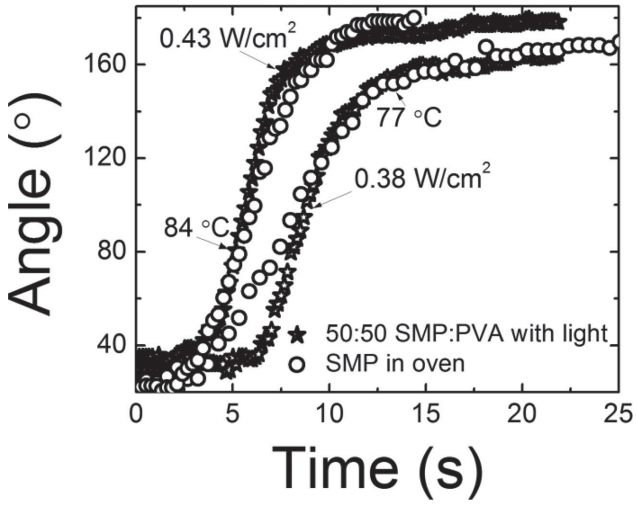

Figure 9. Direct comparison of response on 50:50 SMP:PVA twice-mixed sample (star symbols, intensities given in image for each curve) actuated via photothermal heating and neat SMP heated conventionally (oven temperatures given in image for each curve). The response is almost identical.

3. Conclusion

Blending SMP with a carrier polymer compatible with and containing a desired nanoparticle is a useful approach to enable wavelength-specific light-to-heat triggering for existing shape-memory materials, particularly for specialty applications where accidental triggering must be avoided and/or the surrounding environment is heat sensitive. This scheme is very general (e.g., applicable to magnetic induction heating as well as nanoparticle incorporation for non-heating applications such as tuning of optical or electrical[24] properties) and the associated polymer physics can be well understood. Particles can be contained within polymer that will act as either "soft", "hard", or inert phases with respect to the SMP actuation, with differing advantages and challenges in each case.

In general, actuation response times are determined by the particular heterogeneous temperature distribution within the samples – which is present under both conventional and photothermal heating approaches. Knowledge, measurement, or estimation of the temperature heterogeneity within a sample is necessary to fully understand any photothermal approach where localized heating is important, and is also useful in assessing response under conventional heating. Blending PVA with SMP (at 50:50) resulted in photothermal actuation performance that matched neat SMP with the same transition temperature and response times as when the heat was applied conventionally, provided that the phase size was sufficiently small.

4. Experimental Section

4.1. Materials

Tecoflex EG 72D[25] (polyurethane shape-memory polymer, SMP) was provided in pellet form by Lubrizol. Previous work has determined the glass transition temperature of the soft segment, which should serve as the transition temperature T_{trans} = 74 °C.[19] Citrate-stabilized, spherical gold nanoparticles (AuNPs) were synthesized in-house using the Frens' method,[26] resulting in a water-based suspension. The AuNP particle diameter (determined from transmission electron microscopy images of ≈50 neat particles) was 32 ± 8 nm (standard deviation). Poly ethylene oxide (PEO) (Sigma–Aldrich, 400 kDa) and poly vinyl alcohol (PVA) (Sigma–Aldrich, 126 kDa, 98% hydrolyzed) were used as water-soluble carrier materials into which the AuNPs were incorporated with the resultant composite blended with SMP. The literature value for the T_g for PVA of ≈85 °C was confirmed via differential scanning calorimetry measurements on neat PVA film samples (data not shown). Perylene (Sigma–Aldrich) was utilized to monitor sample internal temperature, as discussed below. All materials were used as received from the manufacturer.

4.2. Sample Fabrication

SMP-only and SMP:PEO (PVA) composite samples were fabricated by placing ca. 4 g of powdered polymer on a preheated melt press (Fred S Carver Inc 2103–2) at 150 °C (210 °C), melting for 1–5 min (45–60 s), and applying 0.3–4.8 MPa for 15–45 s to result in thin film ≈5 cm radius discs having a controllable thickness. AuNPs:carrier polymer (either 0.1 or 0.2 wt%) samples of PEO (PVA) were fabricated by dissolving the polymer in the AuNP solution, stirring at 25 °C for 2–3 d (70 °C for 60 min), and solution-casting onto Parafilm (Pechiney Plastic Packaging) to form a film, which was removed from the paraffin and cut with scissors into approximately 0.3 cm × 0.3 cm squares suitable for cryogrinding. For blends, SMP and PEO (PVA) were individually ground in a liquid-nitrogen cooled cryogrinder (Spex CertiPrep 6750 Freezer/Mill Grinder; 5 min (3 min) precool, five cycles of 2 min (1 min) grinding with 1 min (2 min) cool between cycles) and mechanically mixed by hand for 2 min immediately prior to melt-pressing. Perylene (powder) was added (in the cryogrinder) at a loading that resulted in 0.2 wt% perylene:total mass in each final sample. Twice-mixed samples were fabricated by cutting the postmelt-pressed films into 0.3 cm × 0.3 cm squares, grinding again using the Spex CertiPrep and re-pressing, using previous settings. SMP:PEO (SMP:PVA) samples were prepared at 100:0, 87.5:12.5, 75:25, 62.5:37.5, 50:50, 37.5:62.5, 25:75, and 10:90 (75:25, 66.7:33.3, 50:50, and 10:90). For most experiments, 50:50 SMP:carrier blends with 0.2 wt% (AuNPs:carrier polymer) were utilized with sample thickness of 0.35 ± 0.05 mm (SMP and SMP:PEO) or 0.3 ± 0.05 mm (SMP:PVA). To determine the effect of thickness, pure SMP and 50:50 SMP:PEO samples of 0.1 to 0.5 mm thick were utilized.

4.3. Sample Characterization and Shape-Memory Response

Extinction spectra in the UV to visible wavelength range were measured (Varian Cary 50 Scan UV/Vis Spectrophotometer; (scan

range: 200–800 nm, integration time: 0.125 s)) for 0.1 mm thick samples pressed at 4.8 MPa, which confirmed dispersion of perylene and the AuNPs, and the absence of specific absorption processes due to the various polymers. Phase-segregation within blended materials was characterized by optical microscopy (Nikon Eclipse 50iPOL). Image-J was utilized to quantify phase segregation: a color threshold was set to mark the pixels associated with the non-SMP regions (which were reddish in color when AuNPs were present) and the number of marked pixels was counted to determine the ratio of SMP:polymer. Table 1 summarizes measured areal fraction compared with expected areal fraction for all sample types.

4.4. Shape-Memory Actuation

Samples of 10 mm × 15 mm were cut from the larger films with scissors. The sample thickness was measured and determined to be uniform with a micrometer. Samples were heated to temperatures in the range of 70–91 °C in a conventional oven, set to their temporary shape (folded in half along the long direction), and held while immediately cooled in ambient conditions. The oven temperature was verified using a calibrated Fisher Scientific Traceable Mini-Thermometer ISO 17025. For recovery studies, samples were slightly opened to place a support clip on one side of the folded sample and suspended in air (see Figure 3). The fold was oriented vertically to minimize gravity effects. Upon heating in a conventional oven ("conventional" heating) or at ambient via the photothermal effect under resonant laser irradiation ("photothermal" heating), angle versus time was determined from recorded video observations (Panasonic HDC-TM80) of the first set/recovery cycle. Final open angle (180° for full recovery), quiescent time (the initial time delay after heat is applied before any movement occurs), and characteristic response time (one-half of the time increment between the start and end of motion) were measured using an open-source video-analysis program (Tracker).

Conventional heating trials took place at oven temperatures of 70, 77, 84, or 91 °C. Room temperature samples were placed in center of a preheated oven at $t = 0$ s. The bulk sample temperature as a function of time was measured in control experiments with non-responsive (i.e., not set) composite films in the identical environment via a butt-welded, type T thermocouple (I-Omega) rigidly attached to, and partly inserted into, the folded-over sample. For comparable conditions, the thermocouple results match the average sample temperature determined from perylene probes as discussed below. Reported results are an average from the response of 5–8 specimens per experimental condition.

Photothermal heating utilized a spectrally isolated single line (514 nm) of an argon-ion laser (Coherent, Sabre Innova SBRC-R-ML-14) expanded to a 1.3-cm-diameter spot size that uniformly irradiated the entire sample. Intensity was measured at the sample location (Coherent PowerMax PM10-USB sensor power meter). Internal average temperature was measured as described below. Light intensities were 0.23, 0.30, 0.38, and 0.43 W cm^{-2}, which resulted in average final steady-state temperatures of 66 ± 2, 80 ± 2, 83 ± 2, and 90 ± 3 °C for the 0.1 wt% AuNPs in 50:50 SMP:PEO samples, 71 ± 2, 75 ± 3, 83 ± 2, and 99 ± 2 °C for the 0.2 wt% AuNPs in 50:50 SMP:PEO samples, and 72 ± 3, 81 ± 4, 89 ± 5, and 98 ± 4 °C for the 0.2 wt% AuNPs in 50:50 SMP:PVA samples, respectively. Reported results are an average from the response of 12–15 separate specimens measured at three highest intensities. In all cases, the average temperature was greater than the melting temperature of PEO (T_m = 66 °C); as previously discussed,[5] for these conditions, the final steady-state temperature under photothermal heating is only a weak function of laser intensity and particle concentration. 0.2 wt% AuNPs samples exhibited a more rapid increase in temperature than corresponding 0.1 wt% AuNPs samples up to the PEO melting transition. Samples without AuNPs were separately tested at the same laser intensities; no shape-memory response was observed and the sample temperature was less than 28 °C.

4.5. Fluorescence Temperature Measurement

As previously discussed,[5,12,13] photothermal heating from embedded metal nanoparticles in polymeric systems generates a heterogeneous spatial temperature distribution, with the warmest temperature in the region near the particle. In order to determine the average sample temperature, a molecular thermometer was utilized. The fluorescent molecule perylene has distinct emission peaks in the spectral range of 435 to 550 nm, with the relative intensity of the different emission pathways dependent on temperature (Figure 10). In particular, the amplitude ratio of the peak at ≈480 nm and the adjacent trough (≈465 nm) is essentially linear in temperature over the pertinent temperature range (25–95 °C).[5,27]

Figure 11 shows a calibration curve for 50:50 SMP:PEO sample. This temperature-monitoring technique has been extensively cross-checked against more traditional approaches and serves as the best non-contact approach to monitor temperature in this scenario without interfering with the photothermal process or affecting the SMP response. Under comparable conditions, results

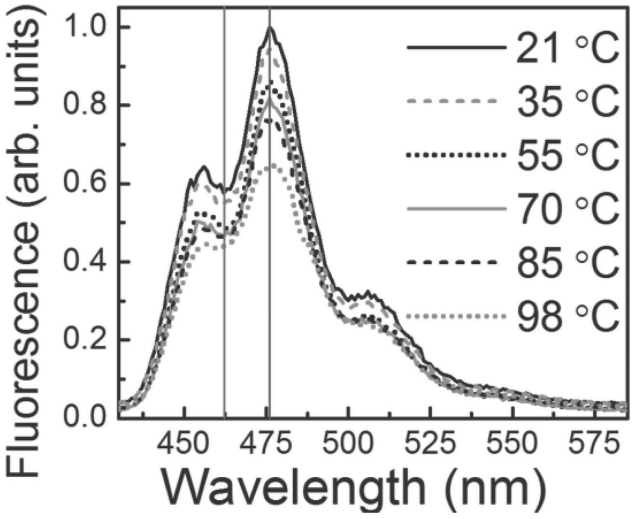

Figure 10. Normalized perylene fluorescence spectra from composite samples at different temperatures under conventional heating. The ratio of the measured amplitude of the 476 nm peak to that of the trough between the adjacent peaks (indicated by vertical lines) provides a quantitative measurement of the bulk temperature.

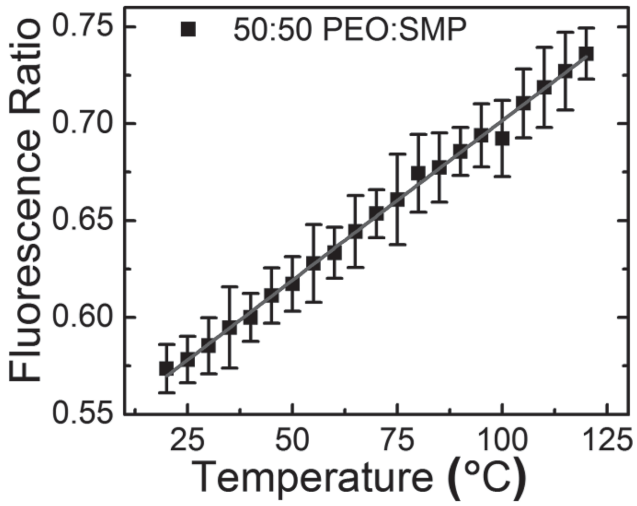

Figure 11. Calibration curve of fluorescence ratio versus temperature (for a conventionally heated, equilibrium temperature, 50:50 SMP:PEO sample in steady-state). The line is a linear fit to the data. Error is determined from measurements of 3–5 samples under identical conditions.

from the perylene technique matched those from a traditional thermocouple. Extinction spectroscopy of samples confirmed dilute molecular absorbance. A fly-wheel chopped (2 kHz), 5 mW, 405 nm blue diode laser with a 5-mm spot size was utilized to excite the perylene. The resulting fluorescence passed through a double-grating scanning monochromator (SPEX 1680B), to a side-on photomultiplier tube detector (Hamamatsu 931B, 800 V) and was photon-counted. Additional experimental details have appeared previously.[5]

Calibration curves were determined by heating using a conventional source. The ratio versus temperature could be well fit by a straight line over the temperature range 20–120 °C. Generally, the fluorescence ratio at a given temperature reflects the non-radiative loss to the polymer (depending for instance, whether the temperature is above or below T_g), with higher ratios indicating greater losses (i.e., more available active motional modes in the polymer).

Acknowledgements: This work was supported by the National Science Foundation (CMMI-0829379, CMMI-1069108), Sigma Xi (GIAR), and an Undergraduate Research Award from NC State University. The authors thank Dr. Vidya Viswanath, Dr. Nagarajan Thoppey, Mrs. Qingqing Wang, Dr. Elizabeth Sacho, Mr. Bruce Anderson, Prof. Albert Young, Prof. Richard Kotek, Ms. Judy Day, Prof. Keith Weninger, the Non-Wovens Institute, and the NC State Physics Education and Research Laboratory (EaRL) for assistance and use of equipment. The authors also thank Mr. Brian Belliveau and Lubrizol for donation of the Tecoflex material.

Received: July 15, 2014; Revised: August 8, 2014; Published online: September 29, 2014; DOI: 10.1002/macp.201400386

Keywords: blends; metal nanoparticles; photothermal heating; polymeric materials; shape-memory materials

[1] A. Lendlein, S. Kelch, *Angew. Chem. Int. Ed.* **2002**, *41*, 2034.
[2] J. Hu, *Shape Memory Polymers and Textiles*, CRC Press LLC, New York **2007**.
[3] J. S. Leng, X. Lan, Y. Liu, S. Y. Du, *Prog. Mater. Sci.* **2011**, *56*, 1077.
[4] N. D. Mankame, P. W. Alexander, A. L. Browne, N. L. Johnson, X. Gao, *US Patent 8,438, 714*, **2013**.
[5] S. Maity, J. R. Bochinski, L. I. Clarke, *Adv. Funct. Mater.* **2012**, *22*, 5259.
[6] K. A. Gall, *US Patent 8,430,933*, **2013**.
[7] N. C. DeBeer, D. R. Kurz, D. A. Ferrera, *US Patent 20030216804 A1*, **2003**.
[8] a) K. C. Hribar, R. B. Metter, J. L. Ifkovits, T. Troxler, J. A. Burdick, *Small* **2009**, *5*, 1830; b) H. J. Zhang, H. S. Xia, Y. Zhao, *J. Mater. Chem.* **2012**, *22*, 845; c) H. J. Zhang, Y. Zhao, *ACS Appl. Mater. Interfaces* **2013**, *5*, 13069.
[9] Z. W. Xiao, Q. Wu, S. D. Luo, C. Zhang, J. Baur, R. Justice, T. Liu, *Part. Part. Syst. Charact.* **2013**, *30*, 338.
[10] D. Habault, H. J. Zhang, Y. Zhao, *Chem. Soc. Rev.* **2013**, *42*, 7244.
[11] a) A. M. Schwartzberg, J. Z. Zhang, *J. Phys. Chem. C* **2008**, *112*, 10323; b) P. K. Jain, X. H. Huang, I. H. El-Sayed, M. A. El-Sayed, *Acc. Chem. Res.* **2008**, *41*, 1578.
[12] S. Maity, L. N. Downen, J. R. Bochinski, L. I. Clarke, *Polymer* **2011**, *52*, 1674.
[13] S. Maity, K. A. Kozek, W. C. Wu, J. B. Tracy, J. R. Bochinski, L. I. Clarke, *Part. Part. Syst. Charact.* **2013**, *30*, 193.
[14] a) R. Mohr, K. Kratz, T. Weigel, M. Lucka-Gabor, M. Moneke, A. Lendlein, *Proc. Natl. Acad. Sci. USA* **2006**, *103*, 3540; b) A. M. Schmidt, *Macromol. Rapid Commun.* **2006**, *27*, 1168; c) J. Thevenot, H. Oliveira, O. Sandre, S. Lecommandoux, *Chem. Soc. Rev.* **2013**, *42*, 7099.
[15] H. Koerner, G. Price, N. A. Pearce, M. Alexander, R. A. Vaia, *Nat. Mater.* **2004**, *3*, 115.
[16] S. Link, M. A. El-Sayed, *J. Phys. Chem. B* **1999**, *103*, 8410.
[17] S. Link, M. A. El-Sayed, *J. Phys. Chem. B* **1999**, *103*, 4212.
[18] U. Kreibig, M. Vollmer, *Optical Properties of Metal Clusters*, Springer, Berlin, Germany **1995**.
[19] C. Schmidt, C. Sarwaruddin, K. Neuking, G. Eggeler, *High Perform. Polym.* **2011**, *23*, 300.
[20] a) N. Y. Choi, A. Lendlein, *Soft Matter* **2007**, *3*, 901; b) X. Lan, Y. J. Liu, H. B. Lv, X. H. Wang, J. S. Leng, S. Y. Du, *Smart Mater. Struct.* **2009**, *18*, 6; c) V. P. Shastri, G. Altankov, A. Lendlein, M. Behl, S. Kamlage, *Advances in Regenerative Medicine: Role of Nanotechnology, and Engineering Principles*, Springer, Dordrecht, The Netherlands **2010**, p. 131.
[21] V. Viswanath, S. Maity, J. R. Bochinski, L. I. Clarke, R. E. Gorga, *Macromolecules* **2013**, *46*, 8596.
[22] H. Zhang, J. Zhang, X. Tong, D. Ma, Y. Zhao, *Macromol. Rapid Commun.* **2013**, *34*, 1575.
[23] G. Kim, A. Wutzler, H. Radusch, G. H. Michler, P. Simon, R. A. Sperling, W. Parak, *J. Chem. Mater.* **2005**, *17*, 4949.
[24] a) C. A. Berven, M. N. Wybourne, L. Clarke, J. E. Hutchison, L. O. Brown, J. L. Mooster, M. E. Schmidt, *Superlattices Microstruct.* **2000**, *27*, 489; b) C. A. Berven, M. N. Wybourne, L. Clarke, L. Longstreth, J. E. Hutchison, J. L. Mooster, *J. Appl. Phys.* **2002**, *92*, 4513; c) L. Clarke, M. N. Wybourne, M. D. Yan, S. X. Cai, L. O. Brown, J. Hutchison, J. F. W. Keana, *J. Vac. Sci. Technol. B* **1997**, *15*, 2925; d) M. N. Wybourne, L. Clarke, M. D. Yan, S. X. Cai, L. O. Brown, J. Hutchison, J. F. W. Keana, *Jpn. J. Appl. Phys. Part 1* **1997**, *36*, 7796; e) M. N. Wybourne, J. E. Hutchison, L. Clarke, L. O. Brown, J. L. Mooster, *Microelectron. Eng.* **1999**, *47*, 55.
[25] C. Guignot, N. Betz, B. Legendre, A. Le Moel, N. Yagoubi, *Nucl. Instrum. Methods Phys. Res. Sect. B* **2001**, *185*, 100.
[26] G. Frens, *Nat. Phys. Sci.* **1973**, *241*, 20.
[27] A. J. Bur, M. G. Vangel, S. Roth, *Appl. Spectrosc.* **2002**, *56*, 174.